Common Mode choke electromagnetic simulation

M. Balestrini, A. Camera

1. EMC competence center, Schurter AG, Mendrisio, TI, Switzerland.

Abstract

Common mode chokes are used in electrical circuits to filter out electromagnetic interference (EMI). The goal of this study is to simulate the impedance of a choke within a range of frequency from 0.01 MHz to 50 MHz.

In this simulation model COMSOL AC/DC Module with magnetic and electric field coupled with electrical circuit setup is used.

The result is very sensitive to relative magnetic permeability μ_r of the used core material throughout its frequency range. Therefore, relative characteristic curves measured in laboratory are imported as a function of frequency into the material properties (in Real and Imaginary parts) and they are used as an input in the magnetic losses magnetization model.

The study starts from Magnetic field Physics, and it considers step by step the influence of skin effect, core conductivity, air volume dimensions, winding geometry, electric field and magnetic permeability, correlated with specific laboratory test measurements.

This toroidal choke model is a first step towards simulating a more complex structure model or a complete EMI filter model.

Keywords: Common Mode Choke, permeability, impedance, inductance.

Introduction

In engineering department it is very important to predict the properties of a choke before realizing a real sample. A 3D FEM simulation model can give the opportunity to optimize a new choke in terms of cost and performance.

Since chokes are an important component within an EMC filter, having a good agreement between a real measurement and a simulated FEM model of a choke is a fundamental starting point for a reliable simulation of an EMC filter.

Theory / Experimental Set Up

Common mode chokes are passive electronic components used to suppress electromagnetic interference (EMI) in electrical circuits. They are designed so that common mode noise, which consists of two unwanted signals flowing in phase on both conductors of a signal or power transmission line, can be filtered out.

Specifically, single-phase common mode chokes consist of two coils wound around a magnetic core. These coils are placed in series with the conductors carrying the signal, thus creating a high impedance path for common mode noise. By introducing this additional impedance, chokes effectively block the unwanted noise while they let the "cleaned" signal to flow.

The primary function of common mode chokes is to reduce EMI and improve the overall performance and reliability of electronic systems. They are commonly used in various applications, including power supplies, data communication systems, audio/video equipment, and industrial machinery. When selecting a common mode choke, factors such as frequency spectrum of the noise to be suppressed, current rating and impedance characteristics should be considered. It is important to choose a choke that matches the specific requirements of the application where it is implemented in, in order to achieve an optimal EMI suppression.

In summary, common mode chokes play a crucial role in mitigating electromagnetic interference in electrical circuits. Their ability to filter common mode noise out makes them an essential component in many electronic systems, ensuring reliable and high-quality signal transmission.

In the context of common mode chokes, core permeability plays a crucial role for their performance. When common mode noise current flows through one coil of a single-phase choke, it induces a magnetic field in the core, which is ideally cancelled out by the magnetic field induced by the noise current flowing through the other coil of the choke.

A core material with a high permeability enhances the effectiveness of this noise reduction. This allows the choke to provide a higher level of attenuation for the common mode noise.

Depending on the specific core material that is chosen during the design of a choke, there are different permeability value ranges. Some commonly used materials include ferrite, iron powder, and nanocrystalline cores. Ferrite cores, for example, have a relatively high permeability up to tens of MHz and they are widely used in common mode chokes due to their excellent magnetic properties and their relatively low cost respect to a nanocrystalline material.

It is important to select a core material with a permeability spectrum that fits on the specific application requirements. Factors such as noise frequency range, the desired level of attenuation and current rating should be considered when choosing the most appropriate core material. Additionally, core geometry and winding configuration also have an impact on the overall performance of the common mode choke.

Equations / Numerical Model / Simulation / Results

The first step of the simulation study presented in this paper has been the creation of an appropriate 3D design of the device under analysis. For this purpose, we chose a vertical choke with a current rating of 40A and we built the corresponding 3D model, where all plastic components were removed since they had no impact on an electromagnetic simulation (Fig. 1). Then we accurately designed the coils to reproduce the actual configuration used in a real sample. Additionally, we defined an outer air volume to enable a comprehensive calculation of magnetic and electric fields surrounding the product.
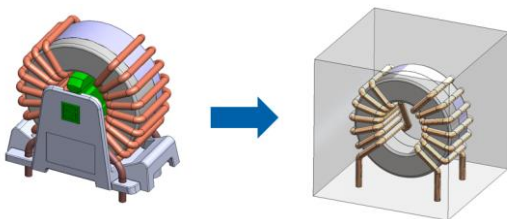

Fig. 1 – 3D CAD model and simulated volume setup.

The Livelink for Solidworks was used to get an easy import of the models.

First of all, the permeability of the material core has been defined in the simulator as a constant parameter, corresponding to the average value between 10 kHz and 100 kHz on the characteristic curve declared by the core manufacturer (Fig. 2).
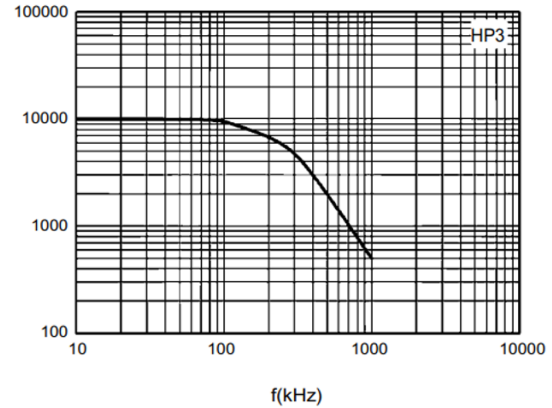

Fig. 2 – Total permeability supplier Datasheet.

The Used Physics is "Magnetic Fields", where a coil domain is inserted. The coil excitation is referred as a simple electrical circuit where input and output resistances are in line with the test setup for the impedance measurement.

The Ampere law domain was set on "Relative permeability" to take as a reference the constant value inserted in core material properties.

To estimate the quality of the output coming from the simulation model, an impedance measurement of the choke has been conducted in our laboratories with a Bode 100 Impedance analyzer (2-ports, 1601 points, Z Mag mode).

As shown in Fig. 3, a pair of choke terminals of the same winding are connected to instrument ports, so that Common Mode impedance can be measured.
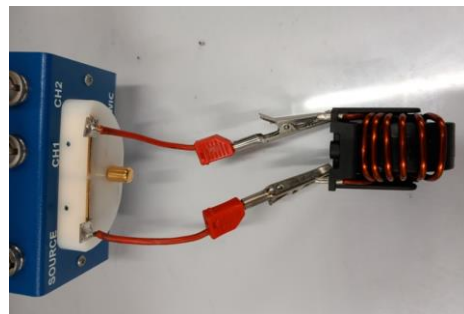

Fig. 3 – Test setup for impedance measurement of the DUT: single-phase ferrite choke.

Measurement is reported in Fig. 4 and its frequency range from 10 kHz to 50 MHz is in line with the operating frequency range of the device.
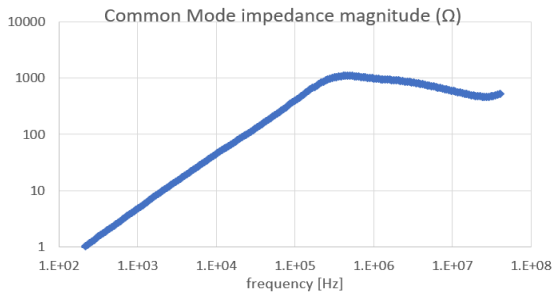
Fig. 4 – Measured Common-Mode impedance.

Fig. 5 shows the measured Common-Mode impedance of the choke, compared to the simulated Common-Mode impedance: it is evident that a good agreement is reached only in the lower region of the spectrum, i.e. up to a frequency of 100 kHz.
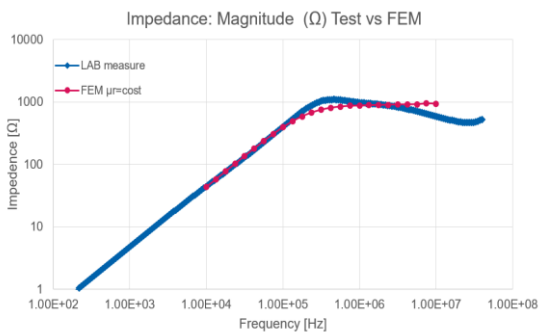

Fig. 5 – Measured Common-Mode impedance (in blue) and Simulated Common-Mode impedance (in red)

The first improvement was therefore to modify the permeability data input by introducing its dependence on frequency in the core material characteristics definition.
The initial definition used was an interpolation function based on values inserted in the relative table derived from the datasheet supplier characteristic curve, as shown in Fig. 6.
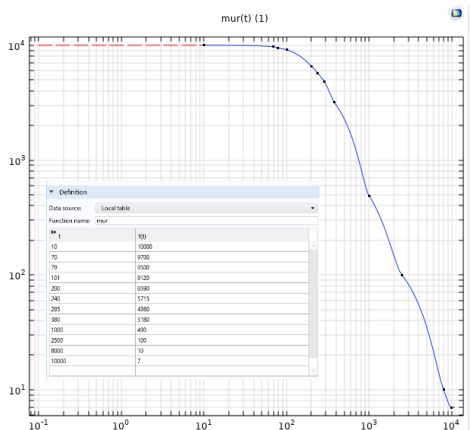

Fig. 6 – µr interpolation curve in COMSOL.

At the same time, among all second-order effects with a possible impact on impedance, we considered the skin effect, as it could play an important role for the simulation of choke impedance.
This electrons rearrangement within wire cross-section implies an additional contribution to choke impedance both in terms of inductance and of resistance.

From a theoretical point of view, with reference to the core under study, skin depth δ varies from 0.65 mm at 10 kHz to 0.02 mm at 10 MHz. This implies a maximum variance of 50 nH/m (according to Fig. 7), that is a negligible contribution to choke inductance.
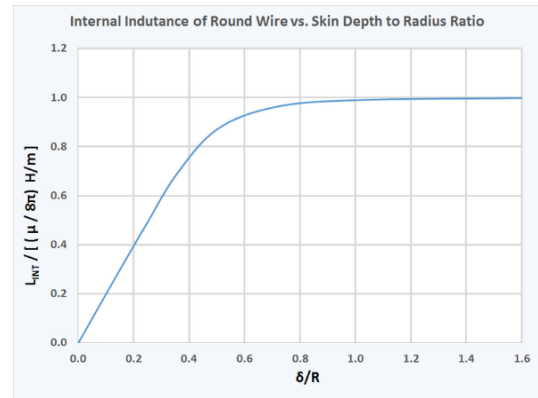

Fig. 7 - Inductance variability due to skin depth

Equation (1) shows the resistive contribution due to skin depth

$$R = \frac{l\rho}{\pi(D-\delta)\delta} \tag{1}$$

Where l is the length of the coil, ρ is copper resistivity and D is wire diameter. Worst case at 50 MHz brings to a contribution of 162 Ω, that is totally negligible respect to measured choke impedance in Fig. 4.

We wanted to consider this effect also in our model, to verify if its contribution is also negligible once compared to simulated Common-Mode impedance.
In order to include this effect, an appropriate new mesh with boundary layer, whose thickness is lower than theorical skin depth has to be created (Fig. 8). A thickness parameter was created as a function of the maximum frequency considered for the analysis.
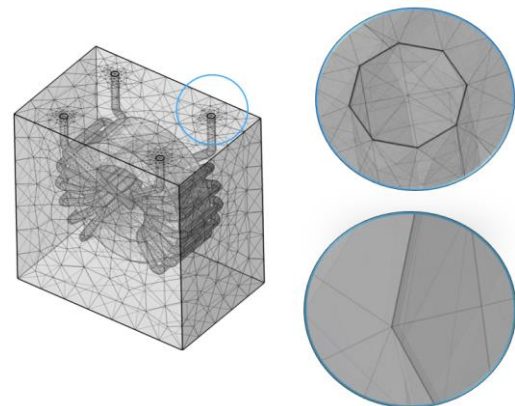

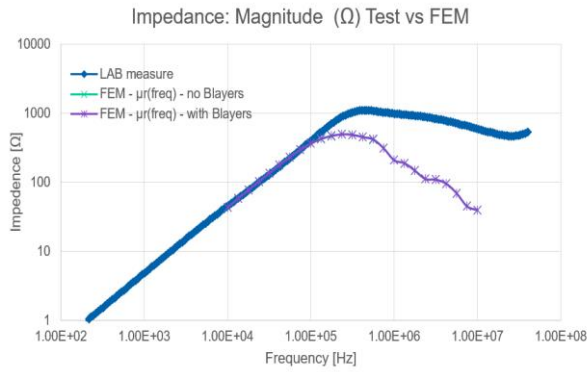*Fig. 8 – Mesh setup with boundary layers.*

Fig. 9 – Measured impedance, variable permeability model setup with and without boundary layer mesh.

Fig. 9 shows an updated comparison between simulation and measurement: the agreement is still poor at medium-high frequency, i.e. from 100 kHz on, while skin effect is negligible, as already demonstrated on a theoretical basis.

Anyway, is evident how permeability values can influence the result at medium-high frequency.
Therefore it was necessary to improve the permeability values definition with a more detailed dataset, extrapolated from manufacturer's datasheet.
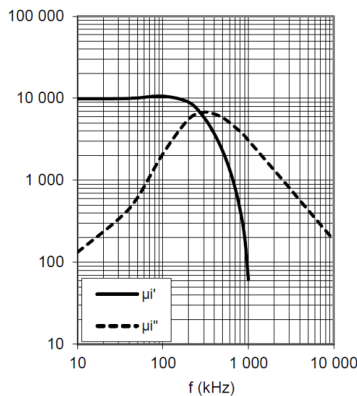

Fig. 10 – Core material real and imaginary relative magnetic permeabilities from manufacturer's datasheet.

The new data in Fig. 10 were in complex format in function of the frequency.
A new magnetization model setup was therefore implemented with "magnetic losses" and with the creation of two functions in the material properties describing the real and the imaginary part, respectively.
A second improvement was to include the electric field in the calculation using the Physics "Magnetic and electric field".
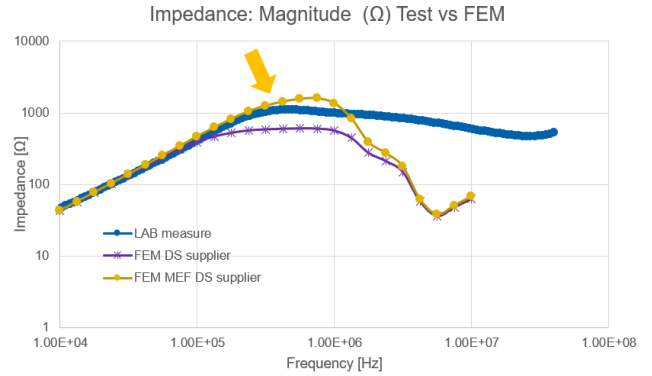

Fig. 11 – Measured impedance, variable permeability model setup with DS supplier data and MEF.

The new model setup results in Fig. 11 fit the measured impedance curve better than in the previous simulation step, also at medium frequencies, i.e. hundreds of kHz.

Another important aspect to be considered is the core conductivity. A value of 5 S/m was considered in material setup.
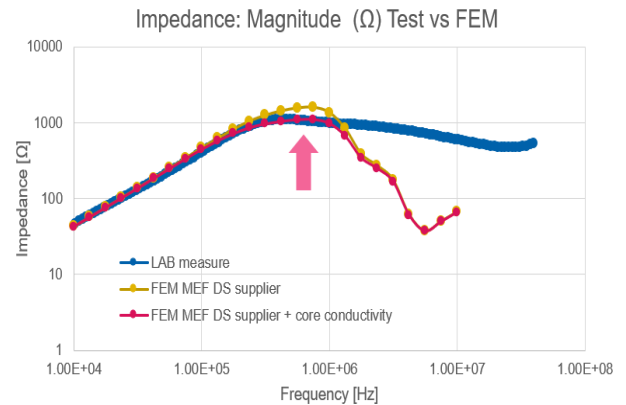

Fig. 12 – Measured impedance, comparison between with and without core conductivity setup.

Core conductivity setup improved results (Fig. 12), since agreement appears to be sufficiently good up to 1 MHz.
To match simulation and measurement beyond this frequency value, we decided to reconsider the quality of permeability data imported into the model.

Even though core manufacturers declare the characteristic curve of magnetic permeability of core materials, shared data are not always sufficient to fully define a complete input dataset for a 3D electromagnetic simulation. In fact, in some cases whether μ_r' , the real part of relative magnetic permeability, or μ_r^{TOT} , i.e. total relative magnetic permeability spectrum, is given. This is in contrast with the need for two separate sets of data, which are μ_r' and μ_r'', i.e. real and imaginary part of relative magnetic permeability of core material.
Furthermore, even though μ_r is almost always indirectly derived by an impedance measurement, manufacturer data are acquired at different test

conditions, in terms of wire cross-section or turns number wound around the core.

All this considered, we opted to conduct measurements in our laboratory and to import these data into the simulation model.
Relative magnetic permeability of a toroidal core with rectangular cross-section is directly proportional to the impedance of the core itself, according to (2)

$$Z = j2\pi f \frac{\mu_0(\mu_r' - j\mu_r'')N^2}{2\pi} c \log_e \frac{b}{a} \qquad (2)$$

where f is frequency, μ_0 is vacuum magnetic permeability, N is the number of turns wound around the core, a, b and c are core geometrical parameters described in the caption of Fig. 13.
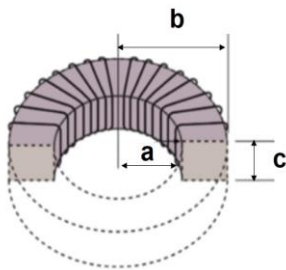

Fig. 13 – Geometrical representation of a core with rectangular cross-section, used as an approximating model of the actual core with toroidal shape. Parameters are outer radius (b), inner radius (a) and height (c).

Impedance analyzers currently used in various company or university laboratories allow to decompose impedance in its real and imaginary parts. Therefore, it is possible to extract real and imaginary parts of relative magnetic permeability by independent equations that can be easily derived from (2).

Relative magnetic permeability derivation from impedance measurement can be affected by some limitations. Although the diameter of the wound wire appears to be negligible, turns spacing has a strong impact on impedance, as it is evident in Fig. 14, where a multiple-turns winding has been broadened with three different opening angles. This implies a splitting of the impedance spectrum at higher frequencies than resonance, due to a capacitive coupling between turns of the coil: the lower the spacing, the higher the coupling.
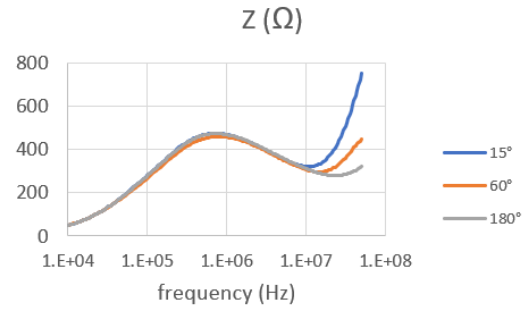

Fig. 14 – Core impedance with three different opening angles of the winding.

In order to minimize this side effect, multiple turns winding should be avoided in favor of a single turn wound around the core, as described in [1]. Furthermore, a large metallic strip should be preferred instead of a thin copper wire, so that inductive parasitics of terminal connections are reduced. This strip should be wound as close as possible to the magnetic material, to reduce the leakage magnetic flux (Fig. 15). In any case, an intrinsic side effect whose impact can't be removed is capacitive coupling between the coil and the core, with a slightly negative contribution to measured permeability at high frequency.
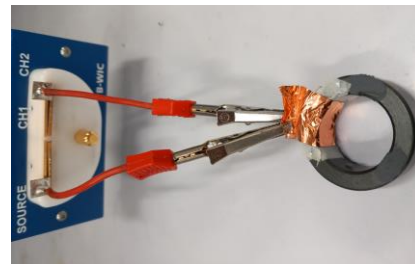

Fig. 15 – Setup for permeability measurement. A metallic strip is wound around the core with a single turn.

Here below (Fig.16) a comparison between relative magnetic permeability measured in our laboratory and the one declared on manufacturer's datasheet is shown.
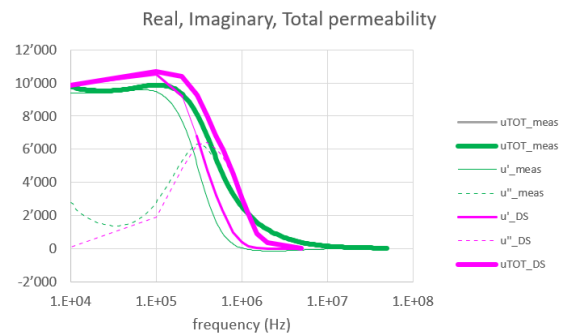

Fig. 16 – Impedance comparison. In green, relative magnetic permeability measured in our laboratory. In purple, relative magnetic permeability declared in manufacturer product datasheet. Real part is in solid line, imaginary part in dashed line, total permeability in bold solid line.

As it is evident by comparing datasheet and measured real permeability and imaginary permeability spectra, there is a significant difference in both cases not only at high frequency, where parasitics are relevant, but also in the lower part of the spectrum.

The last part of the present paper will compare Common-Mode choke impedance from measurement and the one obtained by a simulation with this new permeability dataset, also as a validation of the quality of this new experimental approach.

Furthermore, by measuring cores of different sizes made with the same magnetic material, we noted a huge variability between permeabilities extracted by these sets of data (Fig. 17). This means that there is a significant dependence of permeability on core dimensions and it implies that a single permeability measurement is not representative of the magnetic behavior of cores with the same magnetic material.
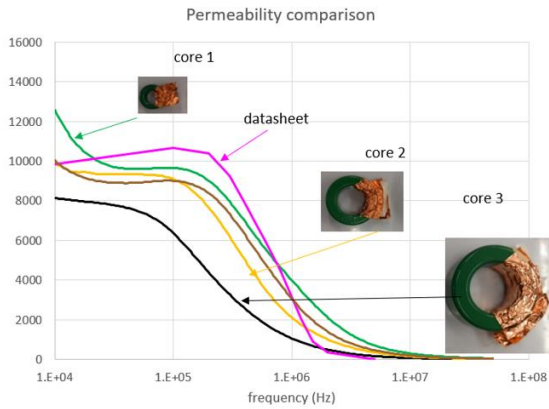

Fig. 17 - Permeability of HP3 cores with different geometries and HP3 permeability from supplier DS.

It was easy for us to format the measurement.xls file in order to directly import it in COMSOL as permeability characteristic functions for the real and the imaginary part, respectively (Fig. 18).
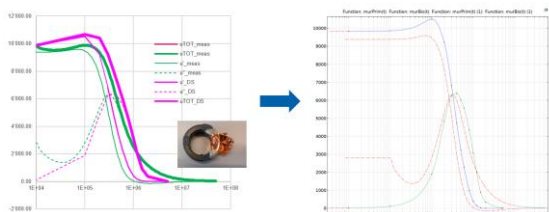

Fig. 18 – Permeability curves comparison imported in COMSOL.

The last model setup has at the end included:
- Magnetic losses
- Magnetic and electric field
- Core conductivity
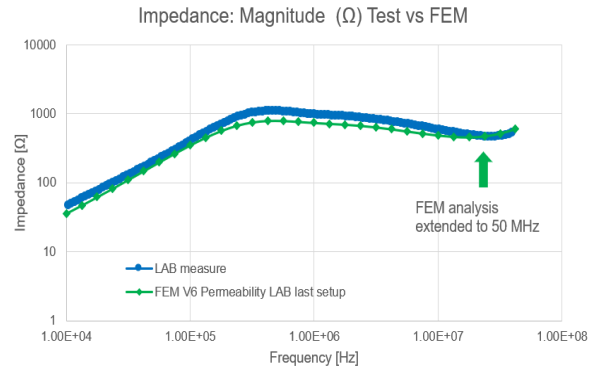- LAB permeability new measurement method

Fig. 19 – Common-Mode impedance curves: measurement (in blue) and COMSOL simulation (in green).

As shown in Fig. 19, the simulation result now is fitting measured Common-Mode impedance in the 10 kHz - 50 MHz frequency range.

Furthermore, COMSOL AC/DC modules allow us to plot magnitude flux lines distribution and magnitude field intensity, as shown in Fig. 20.
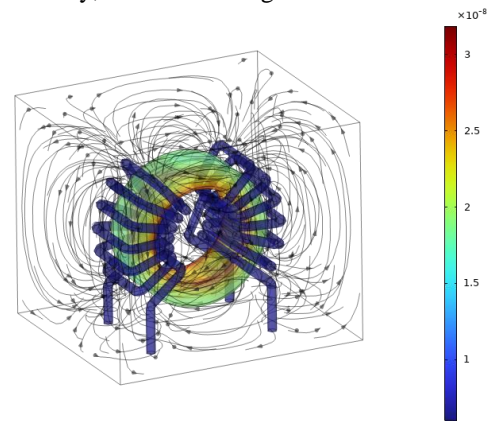

Fig. 20 – Magnetic flux lines in air volume and magnetic field intensity [T] in solid parts @10 MHz.

Conclusions

Throughout this journey, we have come to comprehend the significance of various parameters across diverse frequency ranges. Employing a systematic step-by-step approach has proven to be the correct methodology for the comprehension of possible issues or limitations and to eventually devise effective solutions. The outcomes obtained from this approach now enable us to thoroughly examine all chokes with a reliable model, serving as a foundation for advanced 3D EMC filter simulations.

References

[1] C. Cuellar, W. Tan, X. Margueron, A. Benabou, N. Idir, "Measurement Method of the Complex Magnetic Permeability of Ferrites in High Frequency", in *IEEE International Instrumentation and Measurement Technology Conference Proceedings*, 2012.